Appl Biochem Biotechnol (2012) 167:2341–2356
DOI 10.1007/s12010-012-9729-1

Expression and Characterization of Codon-Optimized Carbonic Anhydrase from *Dunaliella* Species for CO_2 Sequestration Application

Bashistha Kumar Kanth · Kiha Min · Shipra Kumari · Hancheol Jeon · Eon Seon Jin · Jinwon Lee · Seung Pil Pack

Received: 26 February 2012 / Accepted: 3 May 2012 /
Published online: 20 June 2012

Abstract Carbonic anhydrases (CAs) have been given much attention as biocatalysts for CO_2 sequestration process because of their ability to convert CO_2 to bicarbonate. Here, we expressed codon-optimized sequence of α-type CA cloned from *Dunaliella* species (Dsp-aCAopt) and characterized its catalyzing properties to apply for CO_2 to calcite formation. The expressed amount of Dsp-aCAopt in *Escherichia coli* is about 50 mg/L via induction of 1.0 mM isopropyl-β-D-thiogalactopyranoside at 20 °C (for the case of intact Dsp-aCA, negligible). Dsp-aCAopt enzyme shows 47 °C of half-denaturation temperature and show wide pH stability (optimum pH 7.6/10.0). Apparent values of K_m and V_{max} for *p*-nitrophenylacetate substrate are 0.91 mM and 3.303×10^{-5} μM min^{-1}. The effects of metal ions and anions were investigated to find out which factors enhance or inhibit Dsp-aCAopt activity. Finally, we demonstrated that Dsp-aCAopt enzyme can catalyze well the conversion of CO_2 to $CaCO_3$, as the calcite form, in the Ca^{2+} solution [8.9 mg/100 μg (172 U/mg enzyme) with 10 mM of Ca^{2+}]. The obtained expression and characterization results of Dsp-aCAopt would be usefully employed for the development of efficient CA-based system for CO_2-converting/capturing processes.

Keywords Alpha-carbonic anhydrase · Codon optimization · *Dunaliella* species · Inhibitory effects · CO_2 sequestration

B. K. Kanth · K. Min · S. Kumari · S. P. Pack (✉)
Department of Biotechnology and Bioinformatics, Korea University, Jochiwon, Chungnam 339-700, South Korea
e-mail: spack@korea.ac.kr

H. Jeon · E. S. Jin
Department of Life Science, Hanyang University, Seoul 133-791, South Korea

J. Lee (✉)
Department of Chemical and Biomolecular Engineering, Sogang University, Seoul 121-742, South Korea
e-mail: jinwonlee@sogang.ac.kr

Introduction

The accumulation of greenhouse gases, in particular CO_2, in the atmosphere is the main cause for global warming. Earlier in the history, the atmospheric levels of CO_2 were much lower than they are today and could be maintained by forest storage, ocean storage, natural carbonate mineralization, and so on. In the present time, such natural capacity to maintain CO_2 level, however, becomes insufficient for highly increased amount of CO_2 revoked by abrupt industrialization, population growth, energy consumption, and so on. Recently, many researchers have focused on the development of CO_2 sequestration processes, for example post-combustion carbon capture and storage (PCCCS). In this commercial PCCCS processes, various amine-based compounds have been used [1]. Although they have good CO_2 absorption capacities and mechanical stabilities, they have several drawbacks such as corrosion, solvent loss, generation of heat-stable salts, and high-energy consumption during regeneration [2]. Therefore, researchers are now looking for more efficient ways to control the atmospheric CO_2 concentration [3]. In such viewpoint, the biotechnological researchers have also paid much attention to an enzyme-based CO_2 capture system [4] that resembles the naturally occurring CO_2 inter-conversion mechanism in living organisms [5]. This enzyme-based system is expected to contribute to developing an efficient post-combustion CO_2 capture system because enzyme-catalyzed reactions have high chemo-, regio-, and stereo-selective processes [6].

Carbonic anhydrase (CA; EC 4.2.1.1), a zinc containing metallo-enzyme, is such a biological catalyst for reversible hydration of CO_2 ($CO_2 + H_2O \leftrightarrow HCO_3^- + H^+$). CA is important in biological systems because the natural inter-conversion between CO_2 and HCO_3^- (un-catalyzed) is slow at ambient condition. The high efficiency of CA is fundamental to many biological processes like photosynthesis, respiration, pH homeostasis, and ion transport [7]. The enzyme CA has been located in various cellular fractions that serve various physiological and metabolic functions [7]. Presently, CAs are divided into three main classes, α, β, and γ, which have no significant primary sequence identity and are supposed to be evolutionarily independent [8]. The existence of additional δ [9] and ζ classes of CAs have also been reported [10]. Recent reports have revealed that several CA genes from two or even all three known classes are identified even in some prokaryotes or multiple genes from the same class are contained [8].

Many researchers have tried to clone CA genes from several living organisms: humans, vertebrate, plant, fungi, microbes, archea, and so on. Recently, aquatic organisms such as macro/microalgae and aquatic/marine bacteria have been given much attention as a new biological resource to find functionally advanced (or novel) enzymes and proteins. Because aquatic organisms and their biological functions have been evolved under unique conditions such as high salinity, we may acquire more functionalized enzymes, which are not found in living organisms from dry grounds or terrestrials. It could be expected that CA enzymes from halophiles or thermophiles (cloned from aquatic organisms) maintain properly folded structures and/or show functions optimally under extreme salt concentrations [11, 12] or elevated temperature [13].

Until now, there have been several reports for cloning or investigating α-type carbonic anhydrase (aCA) from such halo-tolerant green alga *Dunaliella* species. As expected, most of the reports described that *Dunaliella* species aCA maintains its functionality over nearly the entire range of salinities [14, 15]. However, the acquired amount of purified enzyme fractions is not sufficient or the bacterial recombinant expression/purification systems are not set up well, so that its accurate characterization, especially basic information required for further application, has not been studied yet. In the present work, we focused on high expression and detailed characterization of aCA (Dsp-aCA) from halo-tolerant algae

Dunaliella species (evolutionally close to *Dunaliella tertiolecta*) with the ability to grow under high saline environment (up to 1.5 M NaCl). We constructed codon-optimized sequence of the CA (Dsp-aCAopt) and set up efficient expression/purification system on the basis of *Escherichia coli* recombinant host. Subsequently, we characterized its enzymatic properties in terms of its temperature stability, pH stability, Michaelis–Menten parameters, several inhibition or enhancement factors for CA activity, and so on. Finally, we showed that Dsp-aCAopt enzyme can be employed for CO_2-to-calcite conversion reactions. These results obtained here would be useful for further development of more efficient enzyme-based CO_2-converting/capturing processes.

Materials and Methods

Strains, Plasmids, and Reagents

The *E. coli* hosts XL1-Blue MRF [*Δ(mcrA)182*, *Δ(mcrCB-hsdSMR-mrr)172*, *endA1*, *supE44*, *thi-1*, *recA*, *gyrA96*, *relA1*, *lac*, λ^-, {F^-, *proAB*, $lacI^qZ\Delta M15$, *Tn*10 $(Tc)^r$}] was purchased from Staratagen, and BL21(DE3) [F^-, *omp*T, *hsdS* (r_B^- m_B^-), *gal*, *dcm* (DE3)] and the expression vectors pETDuet-1 were obtained from Novagen (Madison, WI, USA). DNA polymerase (ExTaq) was purchased from TaKaRa. Restriction enzymes were obtained from New England Biolabs. DNase I, ampicillin, $AgNO_3$, $Al(NO_3)_3$, $Ca(NO_3)_2$, $Cd(NO_3)_2$, $Co(NO_3)_2$, $Cu(NO3)_2$, $Fe(NO_3)_3$, $Hg(NO_3)_2$, KBr, KCl, KF, KI, KNO_3, $Mg(NO_3)_2$, $NaHSO_4$, NaN_3, $NaNO_2$, $NaNO_3$, NaSCN, $Pb(NO_3)_2$, $Zn(NO_3)_2$, bromophenol blue, sulfonamide, acetamide, and *p*-nitrophenylacetate were obtained from Sigma-Aldrich Co.; Vernal buffer-5X from Lonza (Walkersville, MD, USA); isopropyl-β-D-thiogalactopyranoside (IPTG) from Duchefa (Haarlem, The Netherlands); and TritonX-100 from Yakuri Pure Chemicals (Osaka, Japan). EDTA-free protease inhibitor (Halt Protease Inhibitor Cocktail) and protein assay reagents were purchased from Thermo Scientific. All the molecular biology reagents and enzymes used in this study were of the highest grade.

Construction of Expression Plasmid Vector

Alpha-type CA gene (Dsp-aCA, Fig. 1a) from *Dunaliella* species (evolutionally close to *D. tertiolecta*) was cloned in T-easy vector. The codon-optimized sequence of Dsp-aCA (Dsp-aCAopt, Fig. 1b) was synthesized by Bionics (Seoul, South Korea) for efficient heterogeneous expression in *E. coli*. The leader sequence was removed and the initiation codon was added. The sequence of Dsp-aCAopt was amplified by PCR with the forward [5′-GAATTCGATGGTGAGCGAACCGCATGAT-3′ (underlined: *Eco*RI site)] and reverse [5′-AAGCTTTCACGCCGCCGCGCCGTTATAG-3′ (underlined: *Hin*dIII site)] primers. The reaction conditions are as follows: 94 °C for 7 min, followed by 30 cycles of 94 °C for 1 min, 45 °C for 1 min and 72 °C for 1 min, and finally 74 °C for 10 min. Amplification reaction volume is 50 μL composed of 0.5 μL of ExTaq Polymerase (2.5 U), 5 μL of 10× ExTaq buffer, 4 μL of dNTP (2.5 mM), 1 μL of forward primer (100 pmol), 1 μL of reverse primer (100 pmol), 1 μL of template (2 μg/mL), and 37.5 μL of ddH_2O. The PCR product was separated by agarose gel electrophoresis and was extracted using PCR extraction kit, Expin™ GEL SV (GeneAll Biotechnology, South Korea). The purified DNA fragment was ligated into pGEM-T Easy vector (Promega, Madison, WI, USA) and introduced into competent *E. coli* XL 1 Blue MRF. Recombinant plasmids were isolated from positive clones using mini-prep DNA extraction kit—Exprep™ Plasmid mini (GeneAll Biotechnology,

Fig. 1 Sequence information of genes and amino acid of carbonic anhydrase. **a** Intact gene sequence of alpha-type carbonic anhydrase cloned from *Dunaliella* species (Dsp-aCA) without leader sequence. **b** Codon-optimized gene sequence of Dsp-aCA (Dsp-aCAopt). **c** Translated amino acid sequences from Dsp-aCAopt; *filled circles* zinc-ligand binding His residues

South Korea), and the insert was confirmed by DNA sequencing. After treatment of *Eco*RI and *Hin*dIII on the mini-prepared plasmids, the fragment of 1611 bp was recovered and subcloned into *Eco*RI–*Hin*dIII site of pETDuet-1 vector (Novagen). The resulting pETD-Dsp-aCAopt expression vector (Fig. 2a) was introduced into competent *E. coli* BL21 (DE3) (Stratagene, USA). Other DNA recombinant methods were performed as described by Sambrook et al. [16].

Expression and Purification of Recombinant Dsp-aCAopt Enzyme

For expression analysis, *E. coli* BL21 (DE3) harboring the pETD-Dsp-aCAopt plasmid was grown in LB medium supplemented with ampicillin (100 μg/mL) on an orbital shaker (180 rpm) at 37 °C. When the OD_{600} of the culture reached a value of 0.6, IPTG was added at a final concentration of 1 mM and the culture was grown for 6 h at 37 °C or for 24 h at 20 °C. Induced culture was harvested by low speed centrifugation, washed and re-suspended in Tris–SO_4 buffer (50 mM, pH 7.6), followed by sonication with Digital Sonifier-250 (Branson Ultrasonic Co., Mexico) for cell breakage. The supernatant and pellet fractions were separated by centrifugation at 12,000 rpm for 30 min at 4 °C and then the protein expression was analyzed by SDS-PAGE (12 % gels) as described by Laemmli [17].

For purification of the recombinant protein, approximately 10 g of pelleted *E. coli* cells from 20 °C culture was suspended in 40 mL of lysis buffer containing Tris–SO_4 (25 mM, pH 7.6), Triton X-100 (0.1 %), and 1 mL of EDTA-free protease cocktail. Cells were thawed in ice-cold water bath, and DNase I, $MgSO_4$, and $ZnSO_4$ were added to the bacterial lysate

(final concentrations—20 μg/mL, 15 mM, and 0.5 mM, respectively). The lysate was spun at 15,000 rpm for 30 min in an ultracentrifuge (Gyrozen 1730MR, Incheon, South Korea) at 4 °C, and the resulting supernatant was subjected to affinity purification. The cell extract was loaded onto Talon resin column (HisPur™ Cobalt Spin Column) pre-equilibrated with equilibration buffer [Na-phosphate buffer (50 mM, pH 7.6) containing NaCl (300 mM)] and eluted with the elution buffer [Na-phosphate buffer (50 mM, pH 7.6) containing NaCl (300 mM) and imidazole (150 mM)] according to company manual. The different fractions having single band corresponding to correct size were collected and dialyzed extensively against Tris–SO_4 buffer (25 mM) containing $ZnSO_4$ (10 μM) and concentrated using Amicon Ultra centrifugal filter (Millipore). The entire purification procedure was carried out at 4 °C. The purified protein was analyzed by SDS-PAGE (12 % gels) as described by Laemmli [17]. Coomassie Brilliant Blue R-250 (Bio-Rad) was used for gel staining and then treated several times by de-staining solution until the proper protein bands appear (Fig. 2b). Protein quantity was determined by a spectrophotometer at 595 nm according to the Bradford method, using bovine serum albumin as the standard [18].

CO_2 Hydration Assay

Two milliliters of veronal buffer (pH 8.2), 0.2 mL of bromethymol blue (0.004 %), 0.8 mL of diluted enzyme, and 2 mL of a CO_2 solution (saturated at 0 °C) were mixed. The time (t_c) interval was determined between the addition of CO_2 solution and the occurrence of a yellow-green color. In the same way, the time interval was recorded without an enzyme solution (t_o). The activity was calculated from the formula given below [19].

$$1\ \text{Wilbur} - \text{Anderson Unit} = (t_o - t_c) / t_c \quad (1)$$

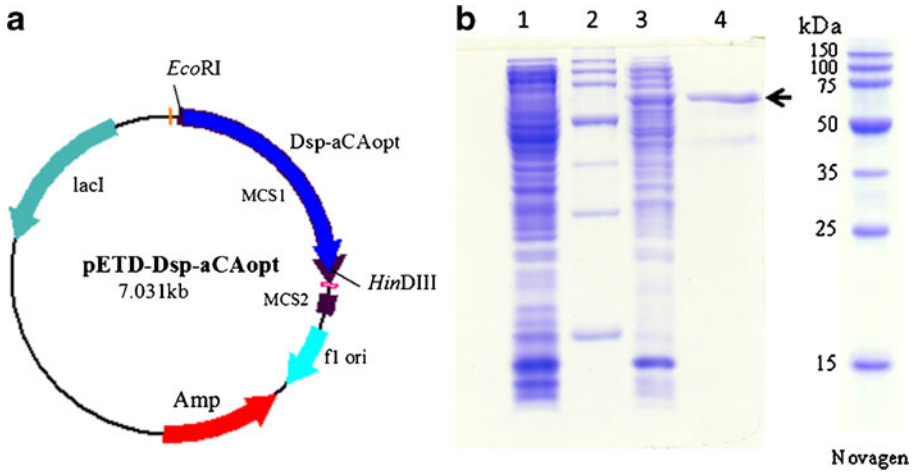

Fig. 2 Expression vector and SDS-PAGE of purified Dsp-aCAopt enzyme. **a** Expression vector, pETD-Dsp-aCAopt: the codon-optimized gene of Dsp-aCAopt cloned in pETDuet-1 at *Eco*RI and *Hin*dIII in multi-cloning site I (MCSI). **b** SDS-PAGE analysis of the Dsp-aCAopt enzyme expressed in BL21(DE3): *lane 1*—crude extract of transformed cell, BL21(DE3):pETDuet-1 (control vector); *lane 2*—molecular mass marker; *lane 3*—crude extract of transformed cell, BL21(DE3):pETD-Dsp-aCAopt (induced with 1 mM IPTG at 20 °C for 24 h); *lane 4*—the purified fraction of Dsp-aCAopt enzyme by affinity-chromatography column (see details in "Materials and Methods")

Esterase Activity Assay

Esterase activity of CA was measured by following the change in absorbance at 348 nm of *p*-nitrophenylacetate (pNPA) to *p*-nitrophenylate ion ($\Delta\varepsilon$=5,000 m^{-1} cm^{-1}) over a period of 3 min at 4 °C using a UV–VIS spectrophotometer (UVmini-1240, Shimadzu Co.) according to the method described by Verpoorte et al. [20]. The enzymatic reaction volume is 3.0 mL composed of 1.4 mL of Tris–SO_4 buffer (50 mM, pH 7.6), 1 mL of pNPA (3.0 mM), 0.5 mL of ddH_2O, and 0.1 mL of enzyme solution. A reference measurement was obtained by preparing the same cuvette without enzyme solution.

Hydration and Sequestration of CO_2

The hydration of CO_2 reportedly involves the transfer of hydrogen ions between the active sites of the enzyme and the surrounding buffer [21]. CO_2-saturated solution used as a substrate was prepared by introducing CO_2 (standard grade) at ~1 bar (100 kPa) into 500 mL of MilliQ grade pure water in a tube with a rubber cork for 1 h at 4 °C. CO_2-saturated solution (10 mL) was mixed with 1 mL of Tris–SO_4 buffer (1.0 M, pH 8.3) containing free Dsp-aCAopt (100 μg) for 15 min. The bicarbonate solution was released into another vessel containing 10 mL of $CaCl_2$ solution (final concentration 10.0 mM). To the mixture, 2 mL of Tris–SO_4 buffer (1.0 M, pH 9.5) was immediately added. The reaction mixture was incubated at 35 and 45 °C, each for 5 min, to allow precipitation of $CaCO_3$. The precipitated $CaCO_3$ was filtered and dried at 60 °C. The resulting $CaCO_3$ was weighed, and the amount of sequestrated CO_2 (gram equivalent of CO_2 present in $CaCO_3$) was calculated [22]. The results were corrected in terms of milligram $CaCO_3$ formed by subtracting the amount from the control experiment carried out in the absence of the enzyme.

Characterizations of Precipitated $CaCO_3$ Solid Crystals

The dry pellets of $CaCO_3$ were subjected to scanning electron microscopy (SEM) and X-ray analysis. Compositions of the precipitated solid crystals were analyzed using X-ray diffraction (XRD) with the Cu Kα radiation (λ=0.154 nm) on a D/Max-2500/PC (Rikaku). The scanning step was 0.02 ° and 2θ ranges from 20 ° to 60 °. The obtained data were compared with the actual XRD data from the Joint Committee on Powder Diffraction Standards. SEM was performed on a JSM7401F (JEOL, Japan) to determine crystal morphology.

Results and Discussion

Expression and Purification of Dsp-aCAopt Enzyme

Intact gene of alpha-type CA cloned from *Dunaliella* species (Dsp-aCA, Fig. 1a) consists of 1770 bp (size of open reading frame). When we carried out multiple alignment with other CAs from similar *Dunaliella* species, the cloned Dsp-aCA was found to have 43 % identity with DCAI (AAF22644) from *Dunaliella salina* and 99 % with dCAI (AAC49378) *D. salina.* We constructed the codon-optimized sequence of Dsp-aCA (Dsp-aCAopt, Fig. 1b) by chemical synthesis for efficient expression in *E. coli.* Here, the leader sequence (first 162 bp toward N-terminus) was removed, and the transcription initiation codon (ATG) was added before codon sequence of 55th amino acid. The codon-optimized Dsp-aCAopt gene (1611 bp) was amplified by PCR and subsequently cloned into pETDuet-1 vector systems

(see details in "Materials and Methods"). In a similar way, we also prepared the expression system of Dsp-aCA gene (noncodon-optimized) using pQE60 vector.

In preliminary attempts, we testified several vector systems such as pQE series and pET series, and also employed several *E. coli* hosts such as *E. coli* BL21(DE3), *E. coli* M15 [pREP4], and *E. coli* SG13009 [pREP4] to successfully express Dsp-aCA gene. Mostly, in the transformed cells with Dsp-aCA gene expression system (noncodon-optimized), the yield of the expressed CA protein as a soluble form was quite low (negligible), even with the insoluble form (Fig. 3a, b, lanes 5–8). To increase the obtained yield of soluble and active Dsp-aCA, we tried to screen the effects of different parameters: growth medium [LB, 2X YT or Super Broth (SB)], IPTG concentrations (0.1–2 mM), growth temperature (20–37 °C), and cell disruption methods (sonication, freezing, and thawing in the presence or absence of detergents such as Triton X-100 and lysozyme). But most of the attempts failed (data not shown), that is, the acquired amount of soluble Dsp-aCA enzyme was still negligible.

In contrast, Dsp-aCAopt gene (codon-optimized) cloned in pETDuet-1 vector (pETD-Dsp-aCAopt, Fig. 2a) was expressed well in *E. coli* BL21(DE3), and the proteins can be obtained as soluble form. The soluble portion of the expressed Dsp-aCAopt is optimized at 20 °C of growth temperature (Fig. 3a, lanes 1–4), while the insoluble portion was increased at 37 °C of growth temperature (Fig. 3b, lanes 1–4). The expressed amount of soluble Dsp-aCAopt enzyme is 27.79 mg/L (at 20 °C under 1.0 mM of IPTG induction). The crude extract of BL21 (DE3) cell expressing Dsp-aCAopt was applied to the affinity column and the differentially eluted fractions were analyzed by SDS-PAGE for optimizing the purification procedures. A protein fraction that was eluted with 50 mM of sodium phosphate buffer (pH 7.6) contained a protein band of ~59 kDa, as expected for the Dsp-aCAopt enzyme fused to the moiety of N-terminal 6× His-tag sequences (see details in "Materials and Methods") (Fig. 2b).

Esterase Activity and CO_2 Hydration of Dsp-aCAopt Enzyme

Alpha-type CAs (α-CA) including Dsp-aCAopt enzyme show esterase activity, which can be measured by using pNPA as substrate. We investigated the kinetic properties in terms of esterase activity of Dsp-aCAopt enzyme considering Michaelis–Menten equation [$V = V_{max} / (K_m + [S])$]. The changes of the reaction rate (V) of the enzyme at 4 °C and pH 7.5 were measured several times according to the concentration of pNPA ([S]). The K_m (M–M constant) and V_{max} (the maximum reaction rate) were obtained by Lineweaver–Burk plotting estimations [23]. Apparent values of K_m and V_{max} were determined as 0.91 mM and 3.303×10^{-5} μM min^{-1}, respectively (K_{cat} value 3.631×10^{-8} min^{-1}). For α-CA from *Oncorhynchus mykiss* (rainbow trout), apparent K_m and V_{max} for pNPA were 0.40 mM and 0.097 μmol min^{-1}, respectively [24]. Similarly, α-CA from *Dicentrarchus labrax* (teleost fish) has 0.44 mM of K_m and 0.025 μmol min^{-1} of V_{max} [25]. For the same α-CA, K_m was reported as 1.60 mM and V_{max} as 0.509 μmol min^{-1} for pNPA hydrolysis [26]. Dsp-aCAopt enzyme has more affinity to pNPA substrate (lower value of K_m), but lower maximum rate (lower value of V_{max}) than the abovementioned CAs.

As shown in Fig. 4, CO_2 hydration activity was measured by pH change as a function of time. By monitoring the time required for the pH of the assay solution to change from pH 8.3 to 7.3, CA enzyme activity was determined. The pH was determined from the absorbance of the reaction mixture using bromophenol blue [19], varying pH 8.3 to pH 6.0. CA activity is expressed in Wilbur–Anderson (WA) units per milligram of protein and was calculated using the formula $[\{(t_0 - t)/t\}/\text{protein(mg)}]$, where t_0 and t represent the times required for the

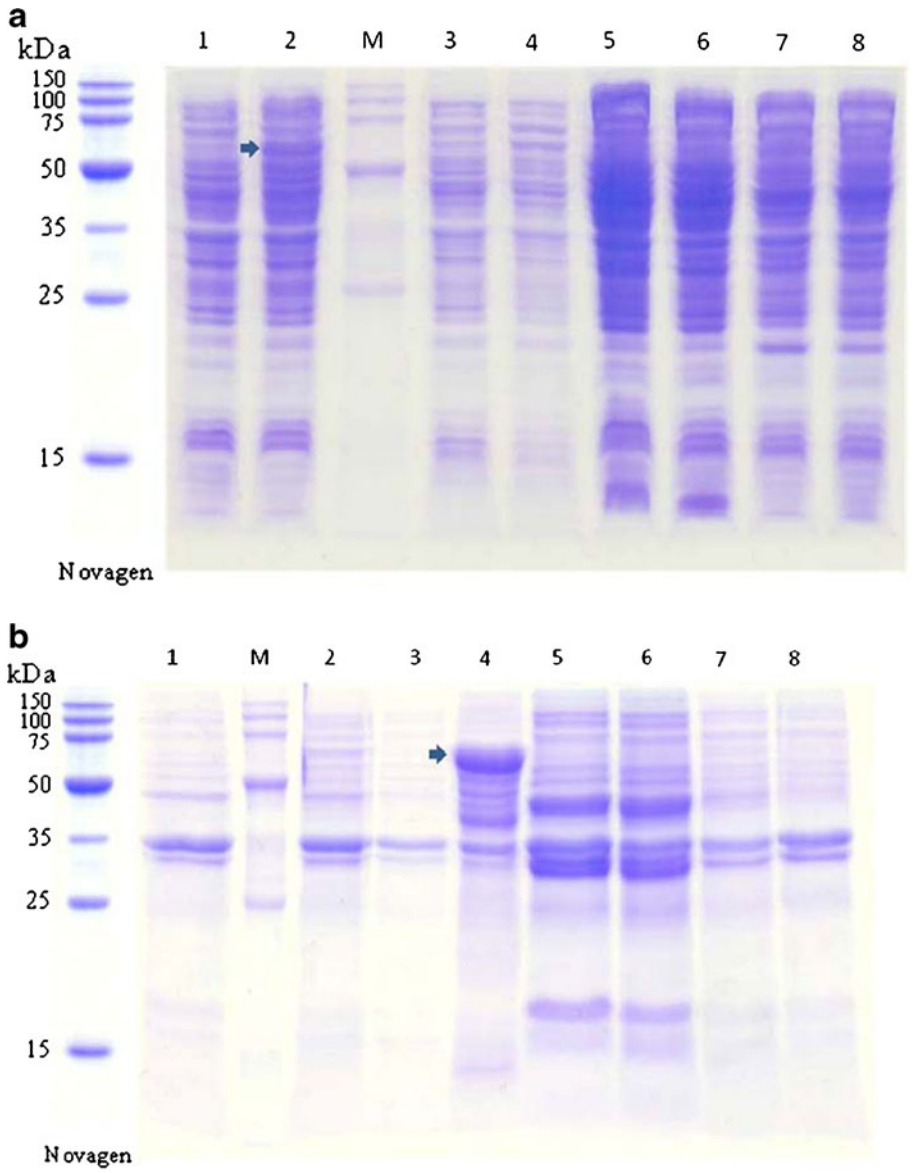

Fig. 3 SDS-PAGE analysis of soluble (**a**) or insoluble (**b**) fractions of Dsp-aCAopt and Dsp-aCA enzymes expressed in *E. coli* BL21(DE3). **a** Soluble fraction in crude extract: *lane 1*—BL21(DE3):pETDuet-1 (control) at 20 °C, *lane 2*—BL21(DE3):pETD-Dsp-aCAopt at 20 °C, *lane M*—molecular mass marker, *lane 3*—BL21(DE3): pETDuet-1 at 37 °C, *lane 4*—BL21(DE3):pETD-Dsp-aCAopt at 37 °C, *lane 5*—BL21(DE3):pQE60 at 20 °C, *lane 6*—BL21(DE3):pQE60-Dsp-aCA at 20 °C, *lane 7*—BL21(DE3):pQE60 at 37 °C, *lane 8*—BL21(DE3): pQE60-Dsp-aCA at 37 °C. **b** Insoluble fraction in crude extract: *lane 1*—BL21(DE3):pETDuet-1 (control) at 20 °C, *lane 2*—BL21(DE3):pETD-Dsp-aCAopt at 20 °C, *lane M*—molecular mass marker, *lane 3*—BL21(DE3): pETDuet-1 at 37 °C, *lane 4*—BL21(DE3):pETD-Dsp-aCAopt at 37 °C, *lane 5*—BL21(DE3):pQE60 at 20 °C, *lane 6*—BL21(DE3):pQE60-Dsp-aCA at 20 °C, *lane 7*—BL21(DE3)pQE60 at 37 °C, *lane 8*—BL21(DE3): pQE60-Dsp-aCA at 37 °C. The expressed bands were pointed out by an *arrow*

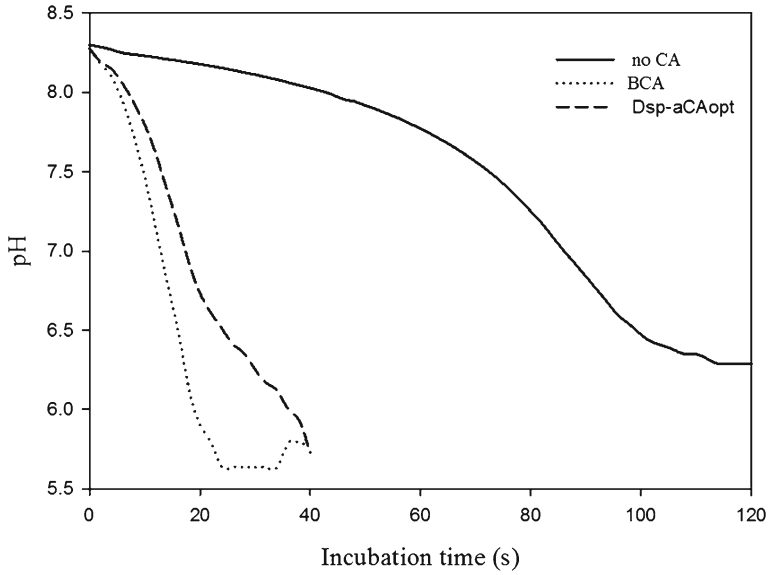

Fig. 4 Plot of pH variation during CO_2 hydration with time. The activity was determined by monitoring the time required for the pH of the assay solution to change from pH 8.3 to 7.3. pH was measured by a change in absorbance of bromophenol blue. *BCA* bovine carbonic anhydrase. Dsp-aCAopt, sequence optimized carbonic anhydrase from *Dunaliella* species under study

pH to change from 8.3 to 7.3 in a buffer control (noncatalyzed) and CA enzyme catalyzed reaction, respectively. Dsp-aCAopt enzyme exhibited a specific activity of 712 WAU/mg proteins.

Effect of Temperature and pH on the Stability of Dsp-aCAopt Enzyme

The temperature denaturation effect on Dsp-aCAopt enzyme was investigated by measuring the residual activity after 1 h of incubation at various temperatures from 15 to 65 °C [Tris–SO_4 buffer (15 mM, pH 7.6)]. There was a rapid decline observed in the activity of Dsp-aCAopt enzyme at the range of 45 to 65 °C. The enzyme was found to retain the same activity at the range of 15 to 35 °C. Only 34.0 % of residual activity was observed at 65 °C compared to that of 25 °C (Fig. 5). The effect of pH on stability of purified Dsp-aCAopt enzyme was investigated in three different buffer systems: 50 mM citrate phosphate buffer (pH 5.0–6.5), Tris–SO_4 buffer (pH 7.0–8.5), and glycine–NaOH buffer (pH 9.0–10.0). The purified enzyme was found to retain 100 % activity at pH 7.6. Interestingly, more than 80 % of enzyme activity was also retained at the range of pH 10.0–11.0, even after 24 h of incubation at 4 °C (Fig. 6). However, 50–70 % activity retained at the range of pH 4.0–7.0. Dsp-aCAopt enzyme shows high stable activity at the two ranges, which are around pH 7.6 and 10.0. The purified Dsp-aCAopt enzyme from *Dunaliella* species was found to be stable at pH range 7.6 and 10. Similar results have been found to be documented. The extracellular CA from *Microcoleus cathonoplastes* showed two peaks of activity at pH 7.5 and 10.0 [27]. In contrast, CA from *Helicobacter pylori* showed high acid tolerance, functioning optimally in the acidic environment of human stomach [28]. All these facts indicate to the remarkable

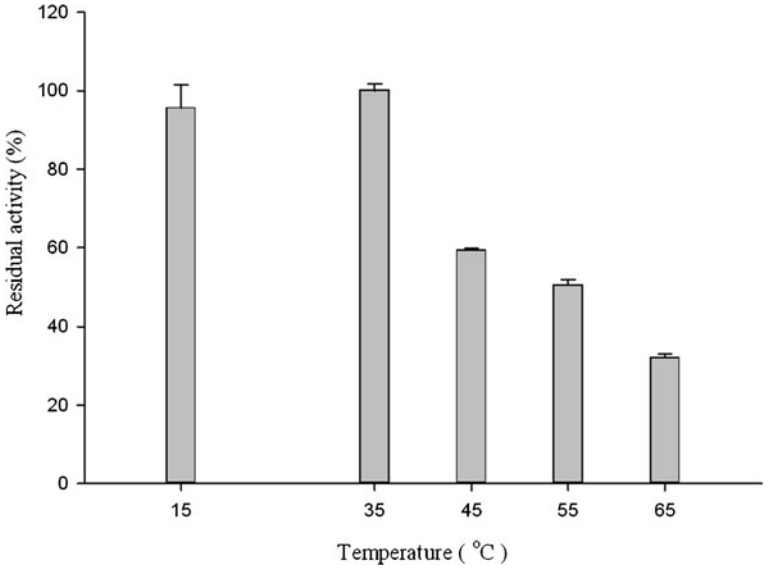

Fig. 5 Denaturation effect of temperature on activity of purified Dsp-aCAopt enzyme. The stability of the enzyme was determined by measuring residual activity after 1 h of incubation at the different temperatures between 15 and 65 °C. The residual enzyme activity was measured according to the standard enzyme assay; 100 % CA activity is equivalent to that of 86 U/mg protein at 25 °C

functional diversity of CA and the ability of this enzyme to perform different roles for the organisms surviving in extreme microenvironments and diverse ecological niche.

Effect of Metal Ions on Dsp-aCAopt Enzyme

At a concentration of 1 mM, the effect of different metal ions on the activity of Dsp-aCAopt enzyme was examined (Fig. 7). Each metal ion individually was mixed with purified enzyme at the ratio of 1:1.35. The activity of Dsp-aCAopt enzyme was stimulated by the addition of Zn^{2+}, Co^{2+}, and Cd^{2+}. It should be noted that all three ions Zn^{2+}, Co^{2+}, and Cd^{2+} are part of the active metal center in different classes of CA [29]; they could have stabilization effects on the catalytic structure of Dsp-aCAopt enzyme, thus enhancing the activity. As shown in Fig. 7, Co^{2+} showed maximum stimulation effect on activity of Dsp-aCAopt. This holds true for most of the alpha-type CAs, where Zn (II) forms the part of the metal coordination sphere [30]. In contrast, the activity of Dsp-aCAopt enzyme was strongly inhibited by Hg^{2+}, Pb^{2+}, and Cu^{2+}. Suppression of CA activity by EDTA suggests that the enzyme is a metalloprotein and/or requires certain metal ions for its activation. Kuhad et al. [31] reported that inhibition due to Hg^{2+} suggests the presence of thiol groups in the active site of the Dsp-aCAopt enzyme. The enzyme activity was not much affected by the presence of Ca^{2+}, Mg^{2+}, K^{+}, and Na^{+} ions, indicating that the Dsp-aCAopt enzyme could perform optimally in the presence of alkaline metals. In α-CA from *Pseudomonas fragi*, similar results have been reported for the metal ion effects. CA activity was stimulated by the addition of Zn^{2+}, Cd^{2+}, and Fe^{2+} ions. CA activity was strongly inhibited by Hg^{2+}, Pb^{2+}, As^{3+}, and EDTA. Enzyme activity was not affected by the presence of Ca^{2+}, Mg^{2+}, K^{+}, and Na^{2+} ions [32]. Dsp-aCAopt is less inhibited by EDTA than α-CA from *P. fragi*. Similarly, α-CA from *D. labrax* (teleost fish) is greatly inhibited by Al^{3+} and Cu^{2+} ions and the order of inhibition was reposted as $Al^{3+} > Cu^{2+} > Pb^{2+} > Co^{2+} > Ag^{+} > Zn^{2+} > Hg^{2+}$ [25].

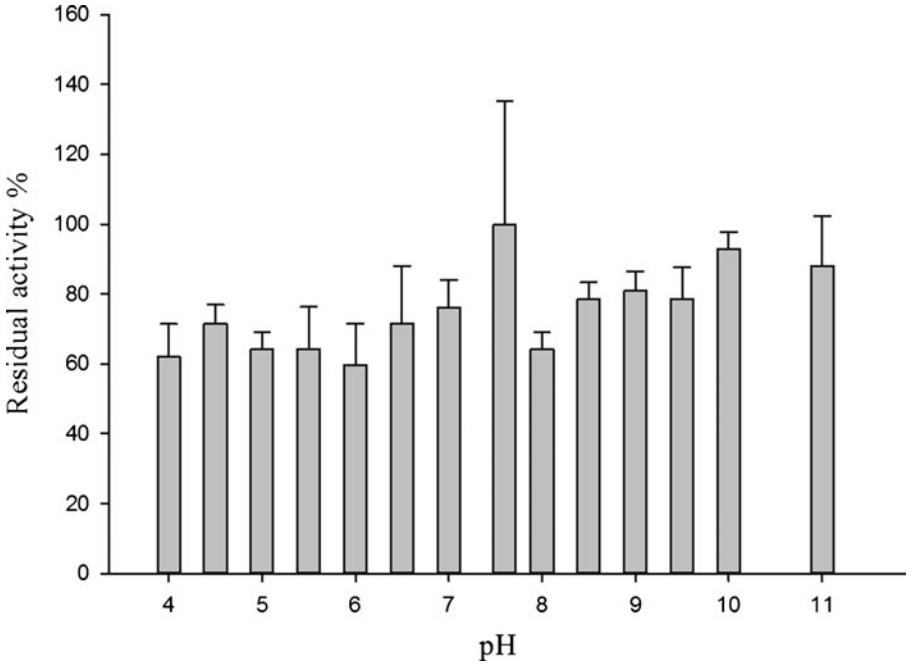

Fig. 6 Effect of pH on stability of purified Dsp-aCAopt enzyme. The pH stability of the enzyme was determined by incubating the enzyme in different pH buffers for 24 h at 4 °C. The residual enzyme activity was measured according to the standard enzyme assay; 100 % CA activity is equivalent to that of 172 U/mg protein

Effect of Inhibitors on Dsp-aCAopt Enzyme

We investigated the inhibition effects of anions or other potent groups on the activity of Dsp-aCAopt enzyme. Acetazolamide, sulfanilamide, and thiocyanate were found to strongly inhibit activity of Dsp-aCAopt enzyme. The inhibitory activity of several anions was observed in the order of $CN^- > SCN^- > F^- > NO_2^- > Cl^- > NO_3^- > SO_4^{2-}$ (Fig. 8). Iodide and acetate have almost negligible inhibition effects. In the cases of inhibition effects, the profile for Dsp-aCAopt enzyme is similar to HCA II, HCA I, and other α-CAs [29]. Both acetazolamide and sulfanilamide were also found to strongly inhibit α-CA from *P. fragi.* The inhibitory activity of the anions was in the order of $CN^- > N_3^- > SCN^- > I^- > NO_3^- > Br^- > Cl^- > SO_4^{2-} > ClO_4^- > F^-$ [32]. Interestingly, N_3^- and Br^- anions showed an enhancing effect for Dsp-aCAopt enzyme activity.

Conversion of CO_2 to Calcite Formation by Free Dsp-aCAopt

$CaCO_3$ has three crystalline mineral polymorphs including rhombic calcite, needle-like aragonite, and spherical vaterite [33, 34]. Calcite is the dominant polymorph at high pH and low temperature and is the most stable at room temperature under atmospheric conditions. While vaterite and aragonite are mostly produced at low pH and high temperature, they can transform to stable calcite [35–37]. Calcite is especially abundant in nature, environmentally harmless, and widely utilized in industry due to its regular crystal size and smooth surface [38]. Carbonic anhydrases have been given much attention as biological

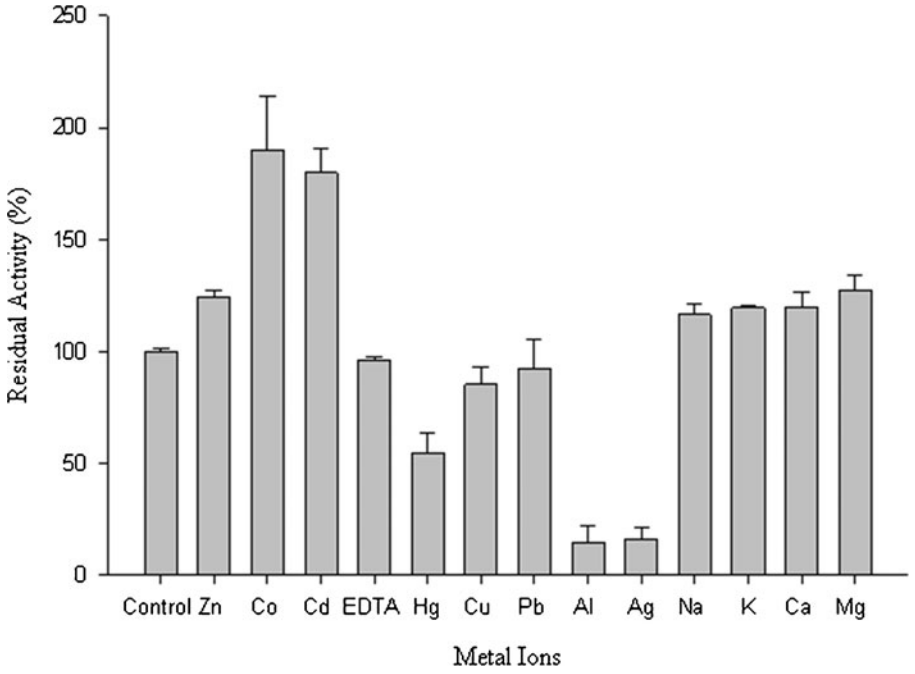

Fig. 7 Effect of metal ions on Dsp-aCAopt enzyme activity. The residual activity of Dsp-aCAopt enzyme was measured after 1 h of incubation of the purified CA enzyme with each metal ion (mixed in ratio of 1.35:1) at 4 °C (control: the activity of Dsp-aCAopt enzyme measured in absence of any metal ion as 100 %)

catalysis for CO_2 sequestration process because the enzyme is known to have the ability to convert CO_2 to bicarbonate. Here, we also investigated the ability of Dsp-aCAopt to mediate CO_2 to $CaCO_3$ formation under Ca^{2+} solution. $CaCO_3$ precipitation using free Dsp-aCAopt enzyme was carried out in Tris–Cl buffer (1.0 M, pH 10.0). $CaCO_3$ was precipitated from the hydrated CO_2 solution by the addition of 4 % $CaCl_2$ solution. The precipitated $CaCO_3$ was recovered by filtration and weighed and the gram equivalent of CO_2 present in the calcium carbonate was calculated. As shown in Fig. 9a, b, FE-SEM image revealed that the morphologies of the $CaCO_3$ crystal obtained by precipitation of hydrated CO_2 (catalyzed by Dsp-aCAopt enzyme) were similar to the morphologies described previously [39]. SEM image revealed rhombohedral calcite crystals. XRD analysis of the precipitated $CaCO_3$ also indicates the formation of a calcite phase (Fig. 9c). The diffraction peaks occurred at 23.07 °, 29.5 °, 36.1 °, 39.5 °, and 43.3 °, corresponding to the calcite crystal faces (012), (104), (110), (113), and (202), respectively, and the representative crystal surface of calcite was 2θ=29.42.

Conclusion

We designed Dsp-aCAopt gene (codon-optimized sequence of alpha-type CA cloned from *Dunaliella* species) and successfully developed its microbial expression system using pETDuet vector and *E. coli* BL21(DE3) [The resulting transformed *E. coli* was named as BL21(DE3):pETD-Dsp-aCAopt]. The half-denaturation temperature of Dsp-aCAopt

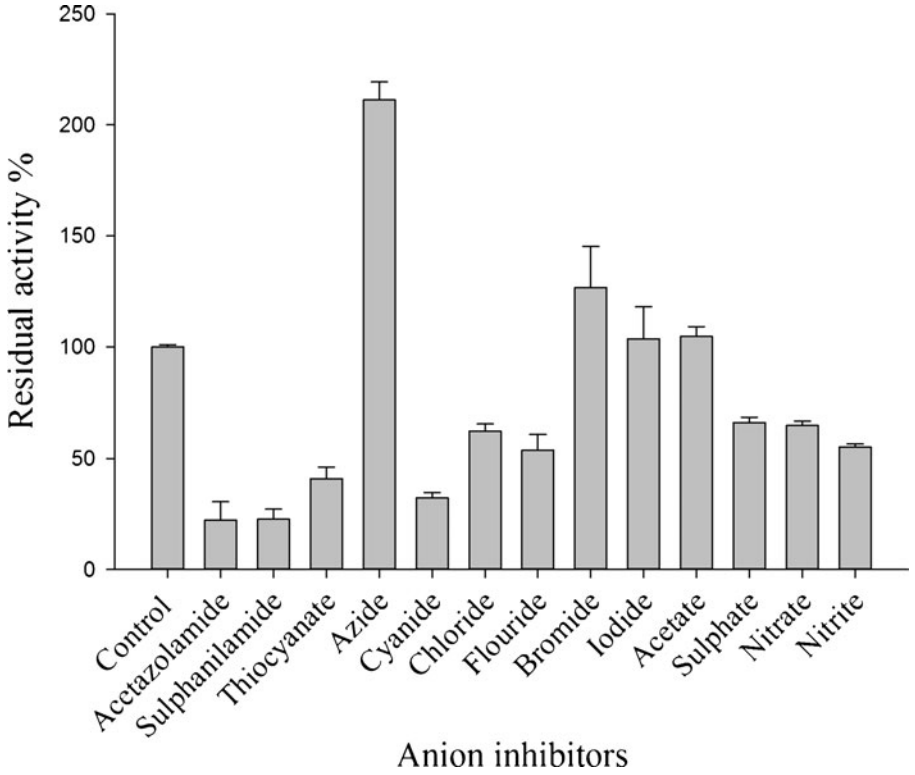

Fig. 8 Effect of inhibitory anions on Dsp-aCAopt enzyme activity. The residual activity of Dsp-aCAopt was measured after 1 h of incubation of the purified CA enzyme with each inhibitor at 4 °C (control: the activity of Dsp-aCAopt enzyme measured in the absence of any inhibitor as 100 %)

enzyme is about 47 °C and the wide pH stability was observed with optimal at pH 7.6/10.0. Alkaline metal ions were found to have a slight enhancement effect on the activity of Dsp-aCAopt with the order of $Na^+ < K^+ < Ca^{2+} < Mg^{2+}$. In the presence of Co^{2+}, Cd^{2+}, and Zn^{2+}, more enhancement effect on activity was observed. However, several metal ions show inhibition effects with the order $Al^{3+} > Ag^+ > Hg^{2+} > Cu^{2+} > Pb^{2+} >$ EDTA. We also investigated the inhibition effects of anions or other potent groups; the order of inhibition effect is as follows: acetazolamide > sulfonamide > $CN^- > SCN^- > F^- > NO_2^- > Cl^- > NO_3^- > SO_4^{2-} > I^-$ > acetate. Interestingly, in the case of Dsp-aCAopt enzyme, Br^- and N_3^- show some enhancement effect on the activity. Finally, we demonstrated that Dsp-aCAopt enzyme can be employed for CO_2-to-calcite conversion reactions.

Until now, there is no report for studying in detail alpha-type CA from *Dunaliella* species. In this study, we made codon-optimized sequence of the CA (Dsp-aCAopt) and set up efficient expression/purification system on the basis of *E. coli* host. In addition, we characterized its enzymatic properties such as half-denaturation temperature, pH stability, Michaelis–Menten parameters, the effects of metal ions, inhibition effects, ability of calcite forming, and so on. These results obtained from this study would be usefully employed for further protein engineering of alpha-type CAs and, finally, for the development of CA-based system for CO_2-converting/capturing processes.

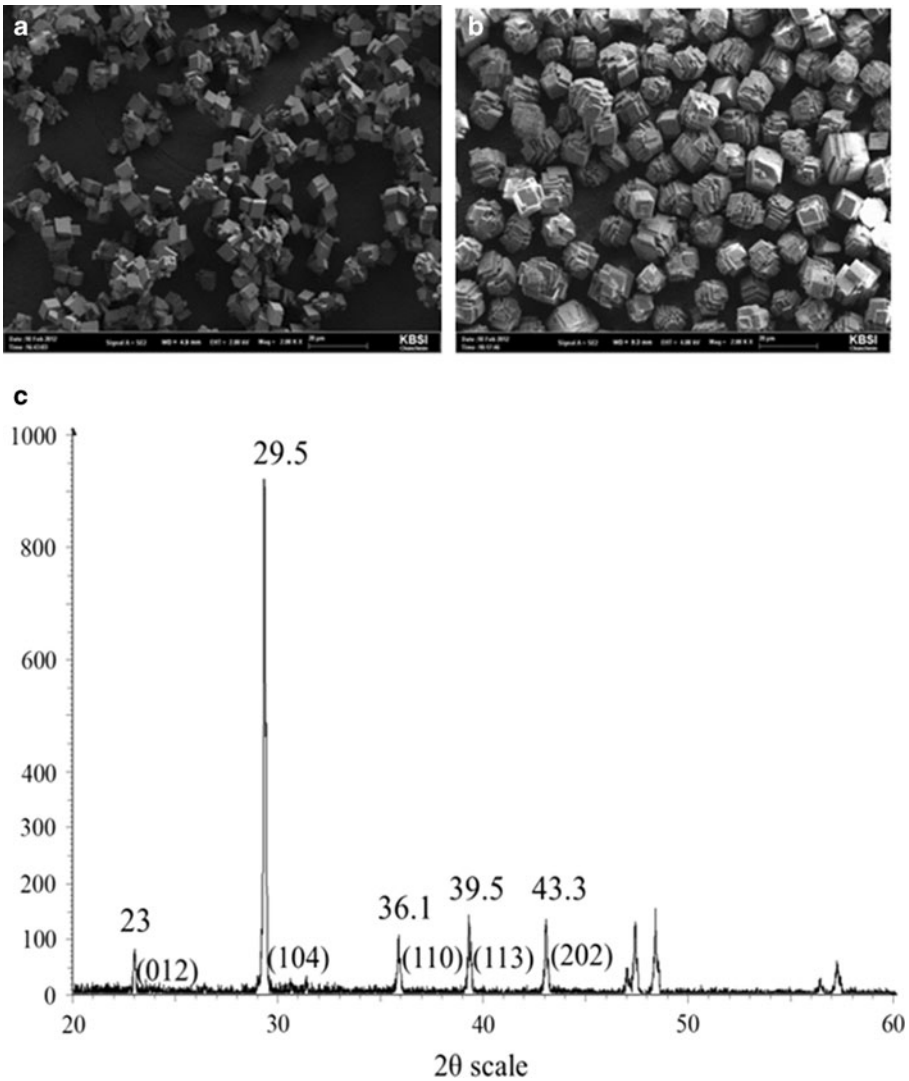

Fig. 9 SEM micrographs of $CaCO_3$ crystals. **a** FE-SEM image of $CaCO_3$ crystals precipitated from naturally hydrated CO_2 (control); **b** FE-SEM image of $CaCO_3$ crystals precipitated from the hydrated CO_2 catalyzed by Dsp-aCAopt enzyme, calcite from (rhombohedral state); **c** XRD spectra of $CaCO_3$ crystals precipitated from the hydrated CO_2 catalyzed by Dsp-aCAopt enzyme

Acknowledgments This work was supported by the National Research Foundation of Korea Grant funded by the Korean Government (MEST) (NRF-C1ABA001-2010-0020501).

References

1. Puxty, G., Rowland, R., Allport, A., Yang, Q., Bown, M., Burns, R., Maeder, M., & Attalla, M. (2009). Carbon dioxide postcombustion capture: a novel screening study of the carbon dioxide absorption performance of 76 amines. *Environmental Science & Technology, 43*, 6427–6433.

2. Veawab, A., Tontiwachwuthikul, P., & Chakma, A. (1999). Corrosion behavior of carbon steel in the CO_2 absorption process using aqueous amine solutions. *Industrial and Engineering Chemistry Research, 38*, 3917–3924.
3. Dawson, B., & Spannagle, M. (2009). *The complete guide to climate change* (1st ed.). New York: Routledge.
4. Lee, S. W., Park, S. B., Jeong, S. K., Limc, K. S., Lee, S. H., & Trachtenberg, M. C. (2010). On carbon dioxide storage based on biomineralization strategies. *Micron, 41*, 273–282.
5. Frommer, W. B. (2010). CO2mmon Sense. *Science, 327*, 275–276.
6. Figueroa, J. D., Fout, T., Plasynski, S., McIlvried, H., & Srivastava, R. D. (2008). Advances in CO_2 capture technology—The U.S. department of energy's carbon sequestration program. *International Journal of Green-House Gas Control, 2*, 9–20.
7. Puskas, L. G., Inui, M., Zahan, K., & Yukawa, H. (2000). A periplasmic, α-type carbonic anhydrase from *Rhodopseudomonas palustris* is essential for bicarbonate uptake. *Microbiology, 146*, 2957–2966.
8. Smith, K. S., & Ferry, J. G. (2000). Prokaryotic carbonic anhydrases. *FEMS Microbiology Reviews, 24*, 335–366.
9. Tripp, B. C., Smith, K., & Ferry, J. G. (2001). Carbonic anhydrase: new insights for an ancient enzyme. *Journal of Biological Chemistry, 276*, 48615–48618.
10. So, A. K., Espie, G. S., Williams, E. B., Shively, J. M., Heinhorst, S., & Cannon, G. C. (2004). A novel evolutionary lineage of carbonic anhydrase (ε class) is a component of the carboxysome shell. *Journal of Bacteriology, 186*, 623–630.
11. Madern, D., Ebel, C., & Zaccai, G. (2000). Halophilic adaptation of enzymes. *Extremophiles, 4*, 91–98.
12. Mevarech, M., Frolow, F., & Gloss, L. M. (2000). Halophilic enzymes: proteins with a grain of salt. *Biophysical Chemistry, 86*, 155–164.
13. Szilagyi, F. A. U. A., & Zavodszky, P. (2000). Structural differences between mesophilic, moderately thermophilic and extremely thermophilic protein subunits: results of a comprehensive survey. *Structure, 8*, 493–504.
14. Borowitzka, M. A., & Borowitzka, L. J. (1988). *Micro-algal biotechnology.* New York: Cambridge University Press.
15. Fisher, M., Pick, U., & Zamir, A. (1994). A salt-induced 60-kilodalton plasma membrane protein plays a potential role in the extreme halotolerance of the alga *Dunaliella*. *Plant Physiology, 106*, 1359–1365.
16. Sambrook, J., & Russel, D. W. (2001). *Molecular cloning: A laboratory manual* (3rd ed.). Cold Spring Harbor: Cold Spring Harbor Laboratory Press.
17. Laemmli, U. K. (1970). Cleavage of structural proteins during the assembly of the head of bacteriophage T4. *Nature, 227*, 680–685.
18. Bradford, M. M. (1976). A rapid and sensitive method for the quantitation of microgram quantities of protein utilizing the principle of protein-dye binding. *Analytical Biochemistry, 72*, 248–254.
19. Rickli, E. E., Ghazanfar, S. A. S., Gibbons, B. H., & Edsall, J. T. (1964). Carbonic anhydrases from human erythrocytes: preparation and properties of two enzymes. *Journal of Biological Chemistry, 239*, 1065–1078.
20. Verpoorte, J. A., Mehta, S., & Edsall, J. T. (1967). Esterase activities of human carbonic anhydrases B and C. *Journal of Biological Chemistry, 242*, 4221–4229.
21. Mirjafari, P., Asghari, K., & Mahinpey, N. (2007). Investigating the application of enzyme carbonic anhydrase for CO_2 sequestration purposes. *Industrial and Engineering Chemistry Research, 46*, 921–926.
22. Sharma, A., & Bhattacharya. (2010). Enhanced biomimetic sequestration of CO_2 into $CaCO_3$ using purified carbonic anhydrase from indigenous bacterial strains. *Journal of Molecular Catalysis B: Enzymatic, 67*, 122–128.
23. Lineweaver, H., & Burk, D. (1934). The determination of enzyme dissociation constants. *Journal of the American Chemical Society, 57*, 658–666.
24. Hakan, S., & Beydemir, S. (2012). The impact of heavy metals on the activity of carbonic anhydrase from rainbow trout (*Oncorhynchus mykiss*) kidney. *Toxicology and Industrial Health, 28*, 296–305.
25. Ceyhun, S. B., Sentürk, M., Yerlikaya, Emrah, Erdogan, O., Küfrevioglu, Ö. I., & Ekinci, D. (2011). Purification and characterization of carbonic anhydrase from the teleost fish Dicentrarchus labrax (European seabass) liver and toxicological effects of metals on enzyme activity. *Environmental Toxicology and Pharmacology, 32*, 69–74.
26. Ekinci, D., Ceyhun, S. B., Sentürk, M., Erdem, D., Küfrevioglu, Ö. I., & Supuran, C. T. (2011). Characterization and anions inhibition studies of an α-carbonic anhydrase from the teleost fish *Dicentrarchus labrax*. *Bioorganic & Medicinal Chemistry, 19*, 744–748.
27. Kupriyanova, E., Villarejo, A., Markelova, A., Gerasimenko, L., Zavarzin, G., Samuelsson, G., Los, D. A., & Pronina, N. (2007). Extracellular carbonic anhydrases of the stromatolite-forming cyanobacterium *Microcoleus chthonoplastes*. *Microbiology, 153*, 1149–1156.

28. Stahler, N. F., Ganter, L., Katherin, L., Manfred, K., & Stephen, B. (2005). Mutational analysis of the *Helicobacter pylori* carbonic anhydrases. *FEMS Immunology and Medical Microbiology, 44*, 183–189.
29. Innocenti, A., Muhlschegel, F. A., Hall, R. A., Steegborn, C., Scozzafava, A., & Supuran, C. T. (2008). Carbonic anhydrase inhibitors: inhibition of the β-class enzymes from the fungal pathogens *Candida albicans* and *Cryptococcus neoformans* with simple anions. *Bioorganic & Medicinal Chemistry Letters, 18*, 5066–5070.
30. Lindskog, S. (1997). Structure and mechanism of carbonic anhydrase. *Pharmacology and Therapeutics, 74*, 1–20.
31. Kuhad, R. C., Chopra, P., Battan, B., Kapoor, M., & Kuhar, S. (2006). Production, partial purification and characterization of a thermo-alkali stable xylanase from *Bacillus sp.* RPP-1. *Indian Journal of Microbiology, 46*, 13–23.
32. Sharma, A., Bhattacharya, A., & Singh, S. (2009). Purification and characterization of an extracellular carbonic anhydrase from *Pseudomonas fragi*. *Process Biochemistry, 44*, 1293–1297.
33. de Leeuw, N. H., & Parker, S. C. (1998). Surface structure and morphology of calcium carbonate polymorphs calcite, aragonite, and vaterite: an atomistic approach. *Journal of Physical Chemistry B, 102*(384), 2914–2922.
34. Ouhenia, S., Chateigner, D., Belkhir, M. A., Guilmeau, E., & Krauss, C. (2008). Synthesis of calcium carbonate polymorphs in the presence of polyacrylic acid. *Journal of Crystal Growth, 310*, 2832–2841.
35. Li, W., Liu, L., Chen, W., Yu, L., Li, W., & Yu, H. (2010). Calcium carbonate precipitation and crystal morphology induced by microbial carbonic anhydrase and other biological factors. *Process Biochemistry, 45*, 1017–1021.
36. Vinoba, M., Bhagiyalakshmi, M., Jeong, S. K., Yoon, Y. I., & Nam, S. C. (2012). Carbonic anhydrase conjugated to nanosilver immobilized onto mesoporous SBA-15 for sequestration of CO_2. *Journal of Molecular Catalysis B: Enzymatic, 75*, 60–67.
37. Kim, I. G., Jo, B. H., Kang, D. G., Kim, C. S., Choi, Y. S., & Cha, H. J. (2012). Biomineralization-based conversion of carbon dioxide to calcium carbonate using recombinant carbonic anhydrase. *Chemosphere, 87*, 1091–1096.
38. Garcia-Carmona, J., Morales, J. G., & Clemente, R. R. (2003). Morphological control of precipitated calcite obtained by adjusting the electrical conductivity in the $Ca(OH)_2$–H_2O–CO_2 system. *Journal of Crystal Growth, 249*, 561–571.
39. Vinoba, M., Kim, D. H., Lim, K. S., Jeong, S. K., Lee, S. W., & Alagar, M. (2011). Biomimetic sequestration of CO_2 and reformation to $CACO_3$ using bovine carbonic anhydrase immobilized on SBA-15. *Energy & Fuels, 25*, 438–445.